Vol 7, Issue 1, 2024 **Impact Factor: 5.355** DOI: https://doi.org/10.31426/ijamsr.2024.7.1.7018

IJAMSR

International Journal of Advanced Multidisciplinary Scientific Research (IJAMSR) ISSN:2581-4281

A Review of Fluid-Structure Interactions in Francis Turbines

Satyam Kumar Mohapatra [1]

Research Scholar, Department of M. Tech Thermal Engineering,
Sri Satya Sai University of Technology and Medical Sciences, Bhopal, M.P, India.

Dr Sachin Baraskar [2]

Research Guide, Department of M. Tech Thermal Engineering,
Sri Satya Sai University of Technology and Medical Sciences, Bhopal, M.P, India.

ABSTRACT

Competitive electricity markets and narrowing profit margins have necessitated the operation of hydraulic turbines, particularly Francis turbines, under increasingly demanding and off-design conditions. To meet these challenges, modern turbine runners are often designed to be lightweight and operate across extended ranges. However, these designs are more susceptible to structural issues, particularly when exposed to flow-induced excitations that may approach the runner's natural frequency, potentially leading to resonance and catastrophic failure. Moreover, sediment-laden flows in many hydropower plants exacerbate these risks by causing surface erosion, altering flow dynamics, and compromising structural integrity. This paper focuses on the fluid-structure interaction (FSI) behavior of Francis turbines under such sediment erosion conditions. It reviews key phenomena including flow-induced excitation, added mass effects, hydrodynamic damping, and blade flutter, with attention to how erosion affects these parameters. Both experimental and numerical studies are discussed, along with the impacts of transient operating cycles—such as frequent load variations and start-stop events—on fatigue life. Finally, the review identifies critical gaps in current research and outlines future directions for comprehensive FSI analysis that integrates the effects of sediment erosion.

1. Introduction

Hydropower remains a critical pillar of renewable energy, contributing approximately 20% of global electricity generation [1]. Among the various types of hydraulic turbines, the Francis turbine is widely used due to its adaptability and efficiency over a broad range of operating conditions. Traditionally, hydraulic turbines are designed to operate at optimal flow conditions where the fluid follows the geometry of the components, minimizing energy losses and enhancing efficiency [2, 3].

IJAMSR
International Journal of
Advanced Multidisciplinary Scientific Research (IJAMSR) ISSN:2581-4281

However, the increasing demand for grid flexibility and economic operation forces turbines to run under off-design steady and transient conditions [4, 5]. These conditions introduce complex flow phenomena that deviate from ideal behavior, significantly influencing the dynamic stability and performance of the turbine [6, 7].

Francis turbines consist of both stationary (guide vanes) and rotating (runner blades) elements, which interact dynamically with the fluid flow. This fluid-structure interaction (FSI) can lead to unsteady pressure fluctuations on the blades, inducing vibrations that may cause fatigue cracking when repetitive stress cycles exceed material limits [8–12]. Over the past three decades, FSI analysis has become an integral part of turbine design, addressing parameters such as added mass, damping, blade flutter, stress concentrations, and fatigue life prediction [13–16].

A critical aspect of FSI analysis in Francis turbines is the accurate estimation of natural frequencies under actual operating conditions. The structural components—crown, band, and twisted blades—are highly coupled, meaning deformation in one part affects the overall vibrational response. In a submerged condition, the natural frequency of the runner can drop by over 50% compared to in-air testing due to the added mass of surrounding fluid [17]. If this reduced frequency aligns with rotor-stator interaction or other excitation sources, resonance can occur, risking blade failure [18].

Further complexity arises under sediment-laden flow conditions. Sediment erosion—common in rivers with high silt content—can lead to localized thinning of blade material, geometric distortion, and surface roughness, all of which alter structural stiffness and flow behavior. These changes exacerbate FSI effects by shifting natural frequencies, increasing stress concentrations, and accelerating fatigue damage [5, 19–24]. Moreover, the industry trend toward lightweight, high-efficiency designs heightens the susceptibility of thin blades to flutter and early-life fatigue failures, particularly under erosive conditions and frequent start-stop cycles.

This paper presents a comprehensive review of fluid-structure interaction in Francis turbines, with a special emphasis on the effects of sediment erosion. It highlights key challenges in analyzing flow-induced excitation, hydrodynamic damping, added mass, and fatigue loading in eroded environments. In light of evolving turbine operation strategies and growing concerns over sediment impact, the paper discusses design implications and the urgent need for more robust FSI analysis methodologies that account for erosive wear. Recommendations for future research and design improvements are provided to enhance the operational reliability and longevity of Francis turbines in sediment-prone regions.

2. Forced Excitation in Francis Turbines under Sediment Erosion Conditions

In hydraulic turbines, particularly Francis turbines, **flow-induced vibrations** are critical for understanding the dynamic behavior of the structure. These vibrations originate from several hydrodynamic phenomena, such as **draft tube vortex ropes, Von Karman vortices, rotor-stator interaction (RSI), turbulence, and cavitation** (see *Figure 1*). Under sediment erosion conditions, the structural integrity of the runner and other components becomes more vulnerable, amplifying the adverse effects of such forced excitations.

International Journal of
Advanced Multidisciplinary Scientific Research (IJAMSR) ISSN:2581-4281

One significant source of forced excitation is the **rotating vortex rope (RVR)**, a helical flow structure that develops in the draft tube at part-load conditions. In Francis turbines with fixed blades, low guide vane angles at part load cause the formation of eddies, which interact with the trailing edge vortices. This interaction produces a swirling flow, creating a central recirculation zone known as the vortex rope. The RVR generates low-frequency pressure pulsations (typically 0.2 to 0.4 times the runner rotational speed) that can be decomposed into rotating and axial (plugging) components [26, 27]. Despite the low frequency, these pulsations induce **cyclic stresses** that may result in **fatigue cracks**, especially in erosion-weakened surfaces.

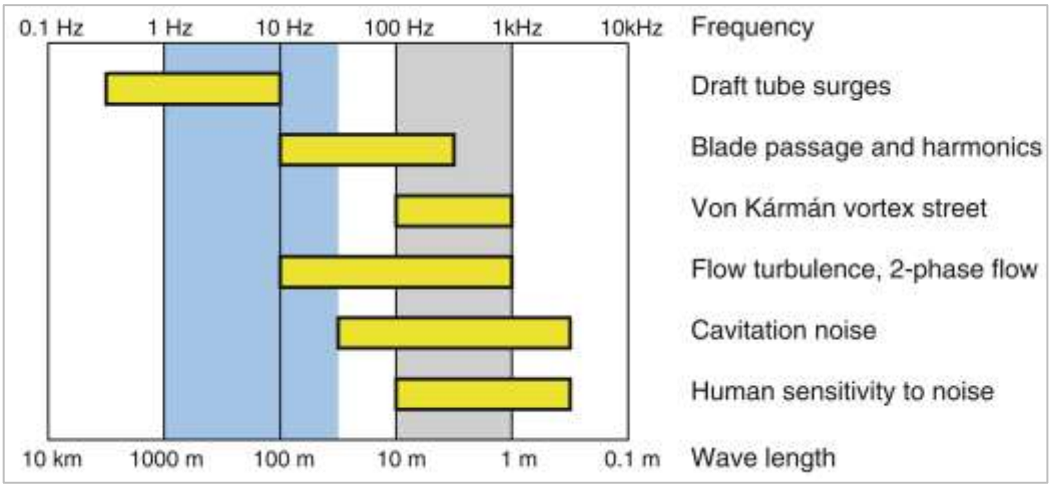

Figure 1: *Overview of the frequencies observed in a hydraulic turbine [30]*

Computational and experimental studies, such as those by Muntean et al. [24], indicate that the **maximum displacement** under vortex rope excitation often occurs at the runner trailing edge near the crown. To control this, air injection is sometimes used, though it may unexpectedly **increase the pressure amplitude** under specific conditions [28]. At higher discharge levels, the vortex core becomes elliptical, and its frequency can rise to five times the runner speed [29, 30]. The cavitation number significantly influences these oscillations, which are more pronounced in model turbines due to scaling effects such as **Froude number dissimilarity**.

Another critical phenomenon is the formation of **Von Karman vortices**, which occur behind the trailing edges of hydraulic components like stay vanes, guide vanes, and runner blades. These are **high-frequency oscillations** linked to the shedding frequency, which depends on the flow velocity and the characteristic length of the component. If this shedding frequency aligns with the **natural frequency of the blade**, a lock-in effect can occur, leading to severe resonance and **structural failure** [31]. Design modifications, such as **oblique trailing edge profiles**, can mitigate these vibrations by weakening vortex cores through alternate vortex shedding and interaction [32].

Rotor-Stator Interaction (RSI) is a dominant source of **forced excitation**, particularly in **mid- and high-head Francis turbines**, where interaction between guide vanes and runner blades produces high-frequency pressure waves (see *Figure 2*). These dynamic pressures can induce **high-cycle fatigue** and, in some cases, **catastrophic blade failure** [10]. Studies show that up to **80% of the**

International Journal of
Advanced Multidisciplinary Scientific Research (IJAMSR) ISSN:2581-4281

total dynamic stress in high-head turbines originates from RSI [8]. Increasing the spacing between guide vanes and runner blades in low-head turbines has been shown to reduce these stresses significantly [33].

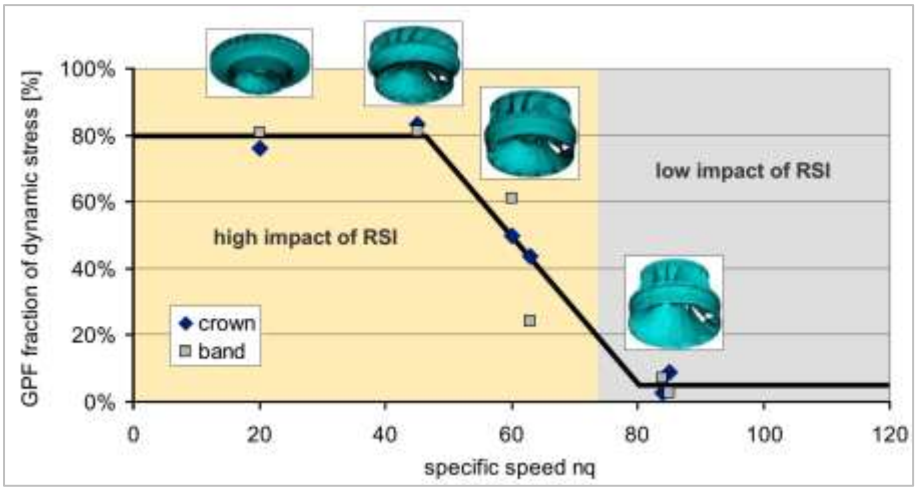

Figure 2: *Level of dynamic stresses caused by rotor-stator interaction in hydraulic turbine [8]*

RSI = rotor-stator interaction frequency, nq = $N \cdot Q^{0.5}/H^{0.75}$, where N = runner speed (rpm), Q = flow rate (m^3/s), H = head (m)

In the context of **sediment erosion**, the already weakened blade surfaces are more susceptible to failure under RSI-induced pressure fields. These interactions can be modeled using **computational fluid dynamics (CFD)**, which can capture both the frequency and amplitude of pressure pulsations (see *Figure 3*). For example, in a high-head Francis turbine, a pressure oscillation at **156 Hz**—close to the natural frequency—was identified, with amplitudes up to **15% of the head** [34].

The RSI frequencies in the stationary and rotating frames are given by:

The rotor-stator interaction frequency and its amplitude can be estimated using CFD techniques [34-36]. **Error! Reference source not found.** shows the dynamic pressure loading on a high-head Francis runner blade. The oscillations correspond to the frequency of forced excitation, 156 Hz, observed in the runner. The amplitudes are approximately 15% of the head. The frequency in the stationary and rotating domains is computed using Equations **Error! Reference source not found.** and **Error! Reference source not found.**, respectively.

$$f_r = n \cdot Z_{gv} \quad \text{(Hz)}$$

$$f_s = n \cdot Z_b \quad \text{(Hz)}$$

where n is the runner speed in revolutions per second, and Z_{gv} and Z_b are the numbers of guide vanes and rotating blades, respectively. The developed pressure field due to rotor-stator interaction is computed using the following equations [35, 37-39]:

Pressure field related to the runner:

IJAMSR

International Journal of Advanced Multidisciplinary Scientific Research (IJAMSR) ISSN:2581-4281

$$p_r = \cos\left(mZ_b\theta_r + \phi_m\right).$$

Pressure field related to the guide vane:

$$p_s = \cos\left(nZ_{gv}\theta_s + \phi_n\right).$$

Combined pressure field:

$$p = A_{mn}\cos\left(nZ_{gv}\theta_s + \phi_n\right)\cos\left(mZ_b\theta_r + \phi_m\right),$$

$$p = A_{mn}\cos[mZ_b\Omega t - (mZ_b - nZ_{gv})\theta + \phi_m + \phi_n] + A_{mn}\cos[mZ_b\Omega t - (mZ_b + nZ_{gv})\theta + \phi_m - \phi_n].$$

Equation **Error! Reference source not found.** is used to determine the pressure field as a function of space and time during rotor-stator interaction. The diametrical mode (*k*) due to rotor-stator interaction is estimated using Equation **Error! Reference source not found.**:

$$k = mZ_b \pm nZ_{gv};$$

where $\theta=\theta_r+\Omega t$, m and n are integers, θ is the angle coordinate, ϕ is the phase angle, A is the amplitude, Ω is the runner angular speed, and t is time. The subscripts “r” and “s” correspond to the rotating and stationary domains, respectively.

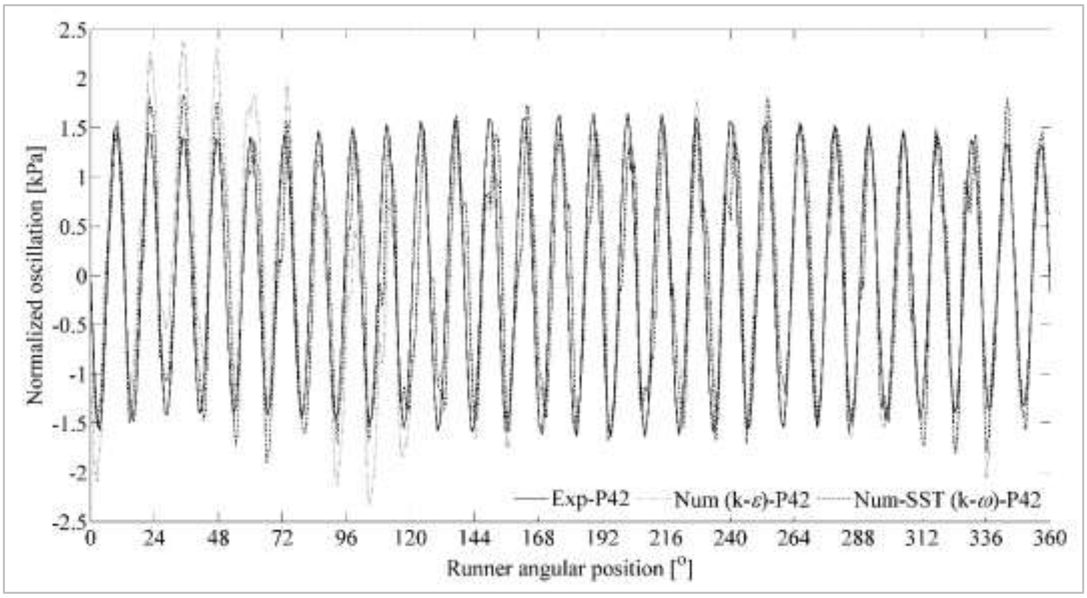

***Figure 3:** Dynamic pressure loading on a Francis runner blade [34]*

(Exp = experimental, Num = numerical; P42 = location of sensor on blade pressure side)

During **steady-state operation**, these forced excitation frequencies remain largely constant. However, during **transient conditions**—such as **start-stop cycles** or **sudden load rejection**—the excitation frequency varies with runner speed and may coincide with the natural frequency of the runner. This **resonance** condition is particularly dangerous in eroded components, leading to further degradation. For instance, during **spin-no-load (SNL)** conditions, **maximum strain amplitudes** have been observed, contributing to both low- and high-cycle fatigue (see *Figure 4*) [40].

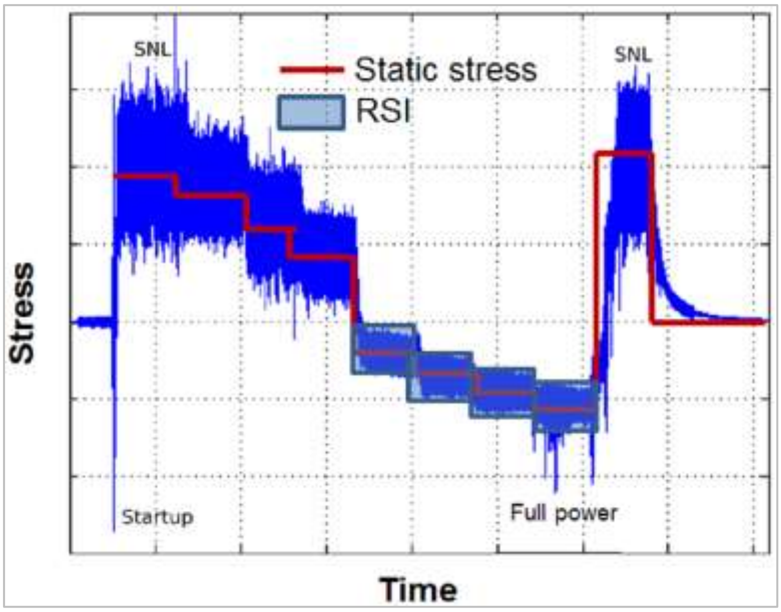

Figure 4: *Strain amplitudes during a complete start-stop cycle of a turbine [40]*

To summarize, **forced excitations**, especially from **rotor-stator interactions**, pose a significant threat to turbine components—more so under **sediment erosion** conditions. While the excitation frequencies and modes can be **predicted during the design phase**, accurately estimating **pressure amplitudes** remains challenging. Errors in amplitude prediction using CFD vary from **10% to 40%** [41], necessitating rigorous **verification and validation** efforts [42–45]. Incorporating sediment erosion effects into these simulations is essential for improving the **accuracy and reliability** of fluid-structure interaction models for Francis turbines.

3. Added Mass Under Sediment Erosion Conditions

3.1 Natural Frequency and Its Significance in Eroded Runners

In fluid-structure interaction (FSI) studies of hydraulic machinery, **added mass** refers to the effective mass a structure acquires due to surrounding fluid inertia when it accelerates. For Francis turbines operating under sediment-laden flow, this effect becomes more complex due to altered flow dynamics and blade surface degradation. The apparent or added mass of a vibrating structure is defined as the reactive hydrodynamic force divided by the acceleration of the structure [46, 47]. It significantly impacts the **natural frequency**, a crucial parameter in assessing dynamic stability and potential resonance.

Added mass is typically determined by computing the hydrodynamic forces acting on the turbine runner and evaluating the structure's deformation corresponding to specific mode shapes [48]. When a runner is submerged in water, the presence of added mass reduces its natural frequency. For runners experiencing **sediment erosion**, the surface roughness and mass distribution are altered, which further modifies these vibration characteristics.

Vol 7, Issue 1, 2024 **Impact Factor: 5.355** DOI: https://doi.org/10.31426/ijamsr.2024.7.1.7018

International Journal of
Advanced Multidisciplinary Scientific Research (IJAMSR) ISSN:2581-4281

Table 1 presents key experimental and numerical studies that highlight changes in natural frequencies due to the added mass effect in Francis turbine runners. These studies serve as a basis for understanding how erosion-induced surface changes can exacerbate or alter added mass behavior. Reductions in natural frequencies ranged from 13% to 64%, with numerical predictions showing deviation from experimental data between 1.5% and 15%, largely depending on the mesh type and density used in simulations. Hexahedral meshes demonstrated better convergence than tetrahedral ones, making them more suitable for erosion-sensitive FSI analysis.

Table 1: *Summary of experimental and numerical studies on added mass in turbine runners under static (non-erosive) conditions.*

Reference	D (m)*	Zb	ν (-)+	ρ (kg/m³)	E (GPa)	Mesh Nodes	Δ#	δ**
[49]	0.4	17	0.56	8300	110	8529/passage	3.6%	39%
[17]	2.9	7	0.27	7700	205	7681/passage	1.5%	58%
[50]	1.3	15	0.34	7700	206	--	12%	48%
	0.7	15	0.39	8600	90	--	15%	64%
[51]	--	9	--	8300	110	165000	12%	13%
[52]	--	13	--	7700	206	20894	3.5%	32%

+specific speed of the runner, $\nu = \Omega\left(Q/\pi\right)^{0.5} / \left(2gH\right)^{0.75}$

*runner outlet diameter

#deviation of numerical value (natural frequency) from the experimental value, $\Delta = 1-(f_{\text{num}} / f_{\text{exp}})$

**frequency reduction ratio, $\delta = 1-(f_{\text{water}} / f_{\text{air}})$

Experimental setups involved runners submerged in still water tanks, excited using impact hammers or piezoelectric patches [53–57]. Measurements were recorded via accelerometers, and their location critically influenced accuracy. For instance, in **Figure 5**, natural frequencies are consistent across P2, P3, and P4 but not at P1 due to its proximity to a nodal point, emphasizing the need for careful sensor placement.

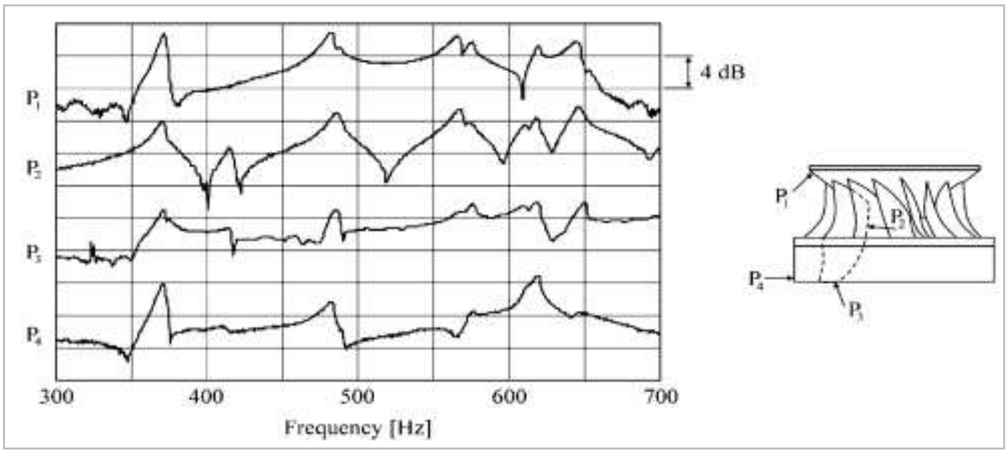

Figure 5: *Frequency response of runner at various accelerometer locations (P1–P4).*

International Journal of
Advanced Multidisciplinary Scientific Research (IJAMSR) ISSN:2581-4281

Note: Improper placement (P1) results in inaccurate readings due to nodal location.

Numerical simulations replicating these experiments utilized fluid-structure coupling with discrete fluid and structural meshes (Figure 6). Hydrodynamic pressure loads from fluid simulations were mapped to the structure for modal analysis. Two approaches were used:

- **Fully coupled simulations** (Figure 7), where fluid and structural solvers iteratively exchange data. These yield high accuracy, especially in cases of **high deformation due to erosion or cavitation**, but are computationally expensive and require fine time steps [60, 61].
- **Sequential coupled simulations**, where flow field and structural response are solved separately. While faster and less demanding, this method assumes negligible feedback from structural deformation to the fluid flow [9].

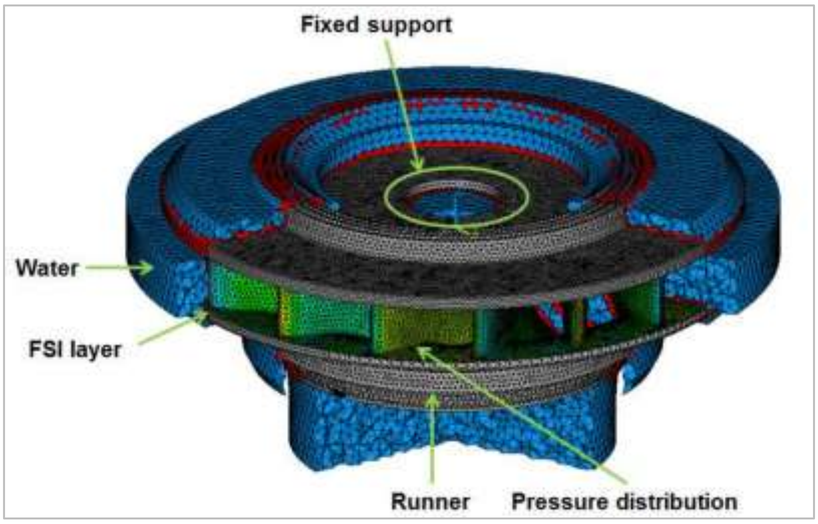

Figure 6: *Fluid-structure mesh of a Francis turbine runner.*

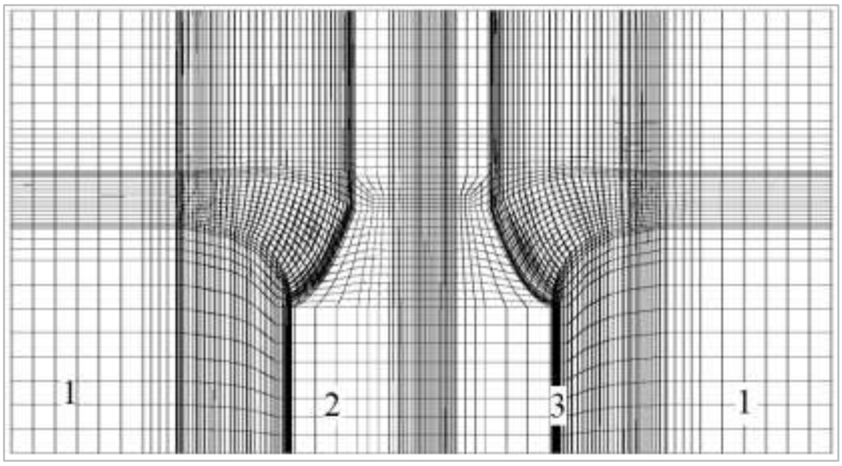

Figure 7: *Example of fully coupled mesh simulation showing conformal interface.*

IJAMSR

International Journal of Advanced Multidisciplinary Scientific Research (IJAMSR) ISSN:2581-4281

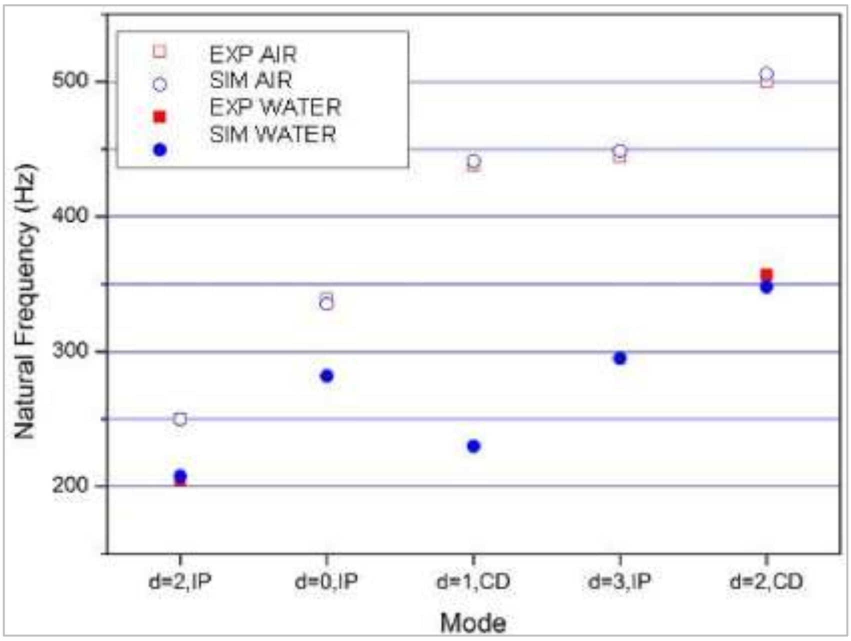

Figure 8: *Comparison of experimental and numerical natural frequencies in air and water.*

Mode shapes (bending, torsion, axial, flexion) play a critical role in added mass analysis. In Francis runners, the greatest frequency reductions occurred in **bending modes**, particularly at five-nodal diameters where frequency dropped by 38% and relative added mass reached 1.64 [53]. Figure 9 highlights mode shape variations in air and water. Mode reordering between media was observed.

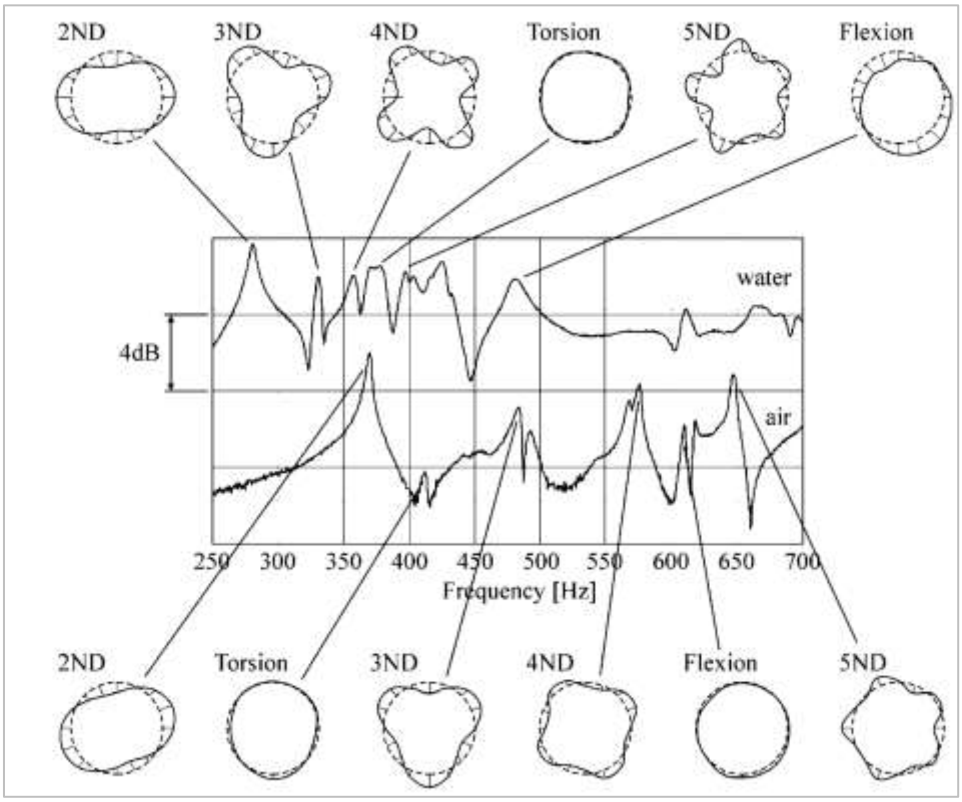

Figure 9: *Observed mode shapes and natural frequencies in model runner (air vs. water).*

IJAMSR
International Journal of Advanced Multidisciplinary Scientific Research (IJAMSR) ISSN:2581-4281

The **cavitation effect**, often exacerbated by sediment erosion, further amplifies the added mass. Tests on hydrofoils (e.g., NACA 0009) demonstrated frequency reductions up to 61% under cavitating conditions (Figure 10). These insights serve as a simplified analog for understanding erosive flow effects in runners.

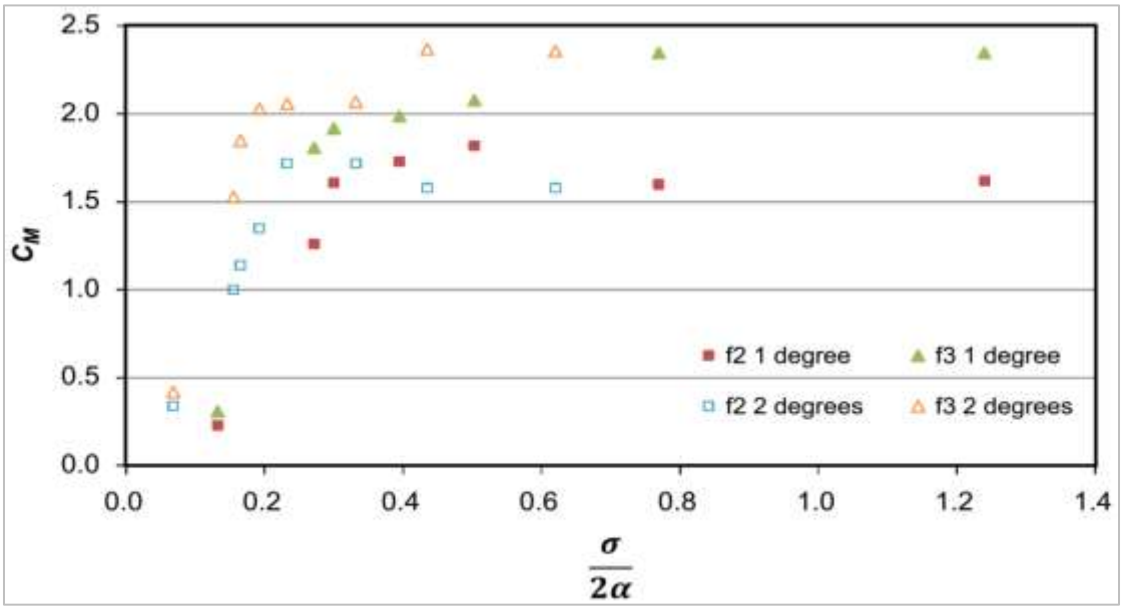

Figure 10: *Cavitation-induced added mass effect on hydrofoil.*

The **interaction between runner components** (blades, crown, band) and nearby structures (seals, vanes, covers) is essential in erosion-prone environments. Deformation characteristics, whether **parallel** or **relative**, influence the added mass significantly. In Figure 11, a 9% effect was seen for parallel deformation at three nodal diameters, while relative deformation at two nodal diameters increased the added mass effect to 37% [58].

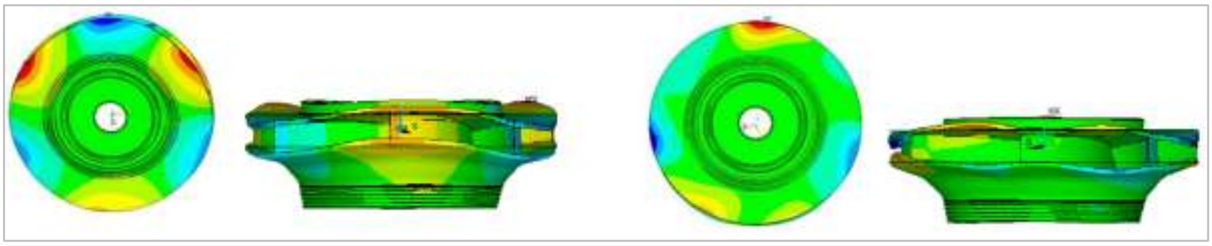

Figure 11: *shows the deformation patterns of a pump-turbine runner at three (left) and two (right) nodal diameters [58].*

During the operation of Francis turbines, the runner undergoes complex interactions with adjacent structural components such as labyrinth seals, guide vanes, distributor rings, and upper and lower covers. The structural response of these components significantly influences the overall dynamic behavior of the runner. Studies indicate that relative deformations, particularly of the band and crown seals, can notably decrease the natural frequencies of the runner system [53, 73–75]. The close proximity of solid boundaries enhances the added mass effect due to pressure buildup and the reflection of pressure waves towards the vibrating runner structure [74, 76].

International Journal of
Advanced Multidisciplinary Scientific Research (IJAMSR) ISSN:2581-4281

Figure 12 illustrates the variation of disc natural frequencies as a function of immersion depth in a fluid tank, with H1=0 mH_1 = 0 \, mH1=0m representing the disc at the free surface and H1=0.16 mH_1 = 0.16 \, mH1=0.16m denoting contact with the tank bottom. As the disc approaches the rigid bottom, natural frequencies rapidly decline, reflecting the added mass dependence on the surface area facing the reflecting boundary [71].

In Francis turbines, the runner is a rotating element, and the added mass effect differs substantially from stationary conditions. Recent experimental investigations on submerged rotating discs rotating at 8 Hz revealed key insights [77, 78]. Four accelerometers positioned at 0°, 90°, 180°, and 210° angular locations captured vibrational responses. **Figure 13** compares the natural frequencies under steady (left) and rotating (right) conditions. The two nodal diameters exhibited natural frequencies at 127 Hz (steady) and 132 Hz (rotating). However, rotation introduced an additional frequency peak at 117 Hz. Similar observations by Hübner et al. [79] attribute this splitting of natural frequencies to standing waves generated by disc rotation.

This analysis highlights three critical points for fluid-structure interaction in rotating Francis turbine runners:

1. The added mass effect on a rotating structure diverges from that under static conditions, with potential for either increase or decrease.
2. Rotational motion induces standing waves, affecting the vibrational spectrum.
3. Nearby surfaces exert strong influence on the natural frequencies.

A key design challenge is the proximity of these standing wave frequencies to forced excitation frequencies arising from runner rotation. Accurate prediction of such frequencies is difficult at the design stage, necessitating comprehensive model testing to estimate potential hydro-acoustic effects across operational speeds.

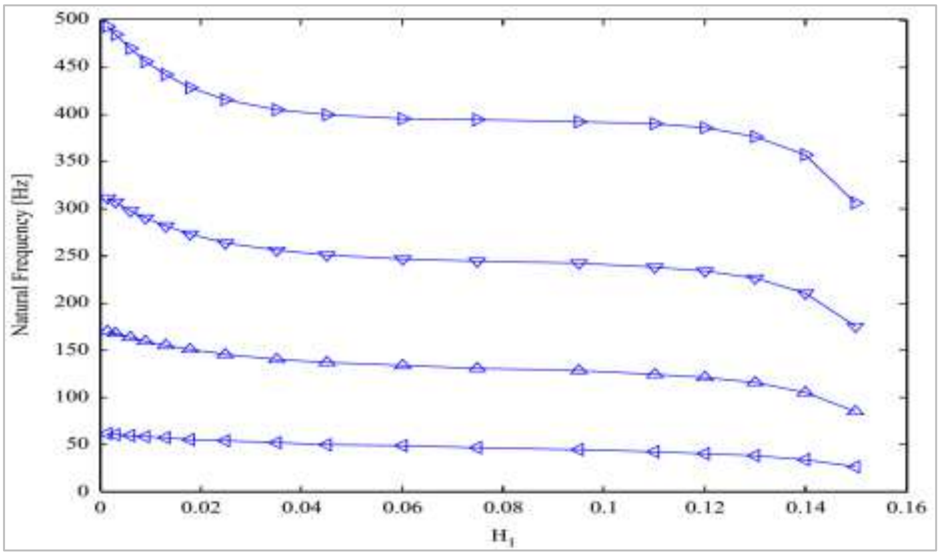

Figure 12 *Effect of immersion depth H1H_1H1 on the disc natural frequency, with natural frequencies near 50, 150, 250, and 450 Hz corresponding to nodal diameters 0, 1, 2, and 3, respectively [73].*

I J A M S R
International Journal of
Advanced Multidisciplinary Scientific Research (IJAMSR) ISSN:2581-4281

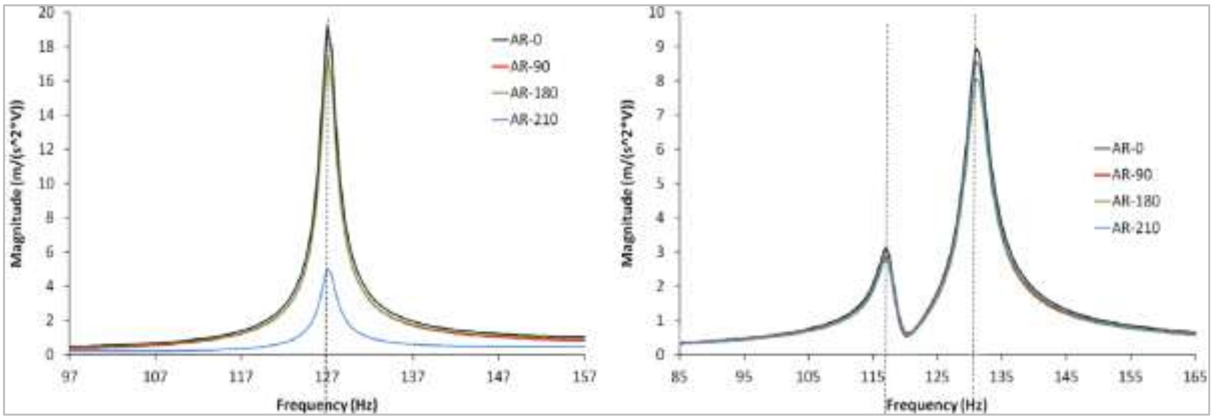

Figure 13: *Added mass effect on a circular disc in water under still (left) and rotating (right) conditions [77]. Accelerometer positions at 0°, 90°, 180°, and 210° are denoted AR-0, 90, 180, 210 respectively.*

3.2 Blade Flutter Under Sediment Erosion and Fluid-Structure Effects

Blade flutter remains a critical issue impacting Francis turbines, especially under sediment-laden flow conditions that exacerbate dynamic loading [80]. Flutter is characterized by self-excited, unstable vibrations driven by unsteady hydrodynamic forces, which can amplify blade displacements exponentially or reach a limit cycle oscillation, risking high-cycle fatigue and structural failure [80, 81]. The presence of multiple blades means that adjacent blade interactions significantly influence flutter mechanisms, primarily through mode shape variations and secondarily via reduced frequencies [82].

Modern turbine runners employ thin, highly skewed blades with complex cross-sectional geometry varying along the blade length. Blade flutter is influenced by several factors: mode shape, reduced natural frequency, fluid velocity, and acoustic resonance within the flow passage [83]. Despite its importance, flutter in hydro turbines is under-researched compared to aero turbines.

Seeley et al. [84] experimentally investigated flutter on a hydrofoil submerged in flowing water up to 22 m/s, using piezoelectric actuators for controlled excitation. Results (Figure 14) demonstrate that vibration amplitude increases with flow velocity; notably, the maximum trailing-edge deflection of 0.05 mm occurred at 70 Hz and 7 m/s flow. Although fluid damping increases approximately linearly with velocity, hydrodynamic forces during flutter can suppress damping, especially under cavitating conditions where vibration amplitudes become pronounced [84]. Experimental replication of these phenomena in Francis turbines is challenging due to the need for high flow velocities (up to 40 m/s) to replicate prototype conditions.

International Journal of
Advanced Multidisciplinary Scientific Research (IJAMSR) ISSN:2581-4281

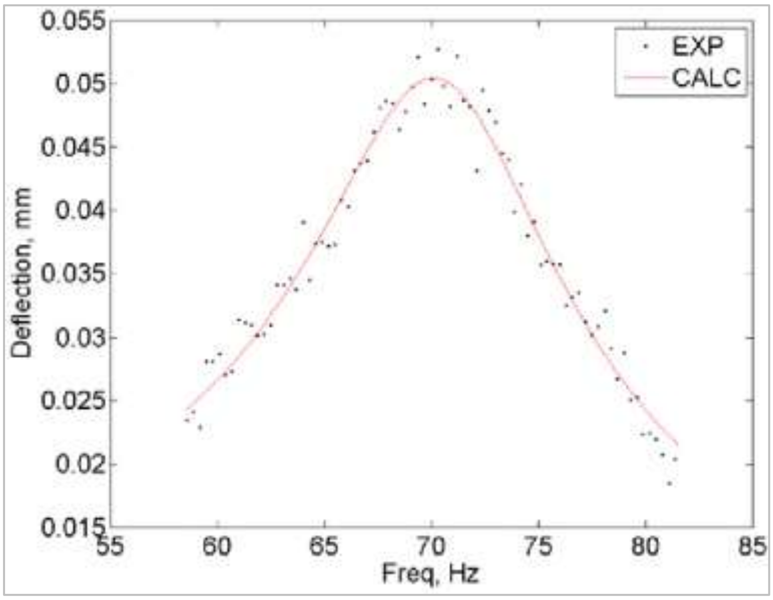

Figure 14*: Hydrofoil deflection under different excitation frequencies at 7 m/s flow velocity [84].*

Recent numerical advances offer promising tools to simulate blade flutter via fluid-structure interaction models [85]. Two primary methods for aerodynamic damping estimation exist: nonlinear time marching and time-linearized analysis [86]. While extensively used for compressible turbomachinery [87–94], their application to hydraulic turbine blade flutter remains limited, representing a valuable research opportunity. Numerical challenges include achieving solution convergence and selecting optimal time-step sizes to capture coupled fluid-structure dynamics accurately.

3.3 Hydrodynamic Damping in Francis Turbines with Sediment Interactions

Added mass and hydrodynamic damping critically govern vibration amplitudes in fluid-structure interaction scenarios within Francis turbines. Large vibration amplitudes can cause fluid detachment from the runner surface, transitioning the fluid-induced force from inertial added mass to damping [16]. Hydrodynamic damping acts as a natural vibration suppressant, particularly important during resonance conditions [95].

Industrial research increasingly focuses on hydrodynamic damping in high-head Francis turbines, especially near resonance [96]. Experimental work on hydrofoils demonstrates that damping ratios increase with flow velocity, albeit with natural frequencies decreasing slightly compared to air measurements [55, 84, 97]. Figure 15 presents the mounting arrangement for hydrofoils and damping ratio trends observed for three geometrically different hydrofoils (H0, H1, H3). At 22 m/s, damping ratio peaks, highlighting velocity dependence, although geometric differences slightly affect the rate of increase.

IJAMSR
International Journal of
Advanced Multidisciplinary Scientific Research (IJAMSR) ISSN:2581-4281

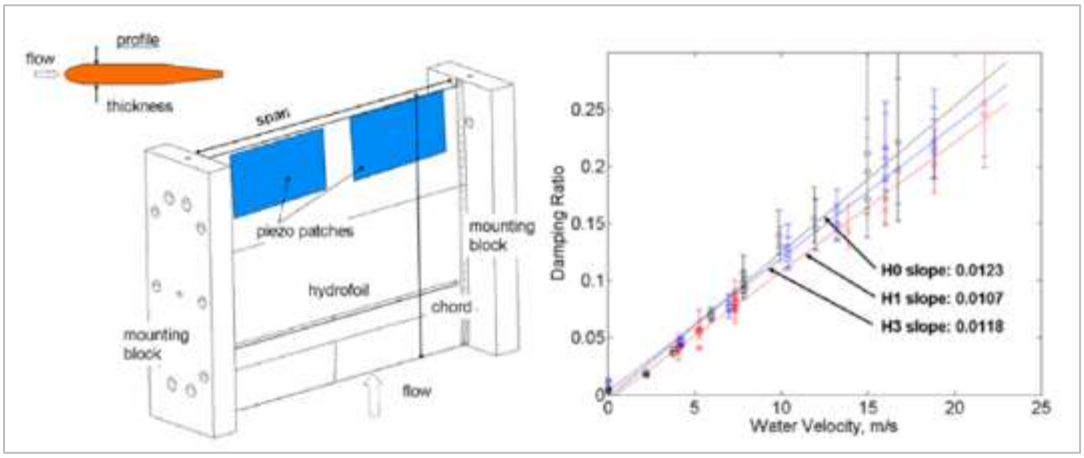

Figure 15: *Hydrofoil mounting and piezoelectric actuator placement (left) and damping ratio variation with flow velocity (right) [Coutu et al., 2012].*

Figure 16 illustrates damping effects for a scaled pump-turbine runner model, showing decreasing damping ratios with increasing natural frequency. Maximum damping ratios were 3.1% in air and 4.1% in water [54]. Notably, low-frequency ranges (~700 Hz) show higher damping but insufficient to suppress flutter amplitudes fully. The excitation frequency range typical for Francis turbines is 100–300 Hz, emphasizing the need for damping evaluation within this operational window.

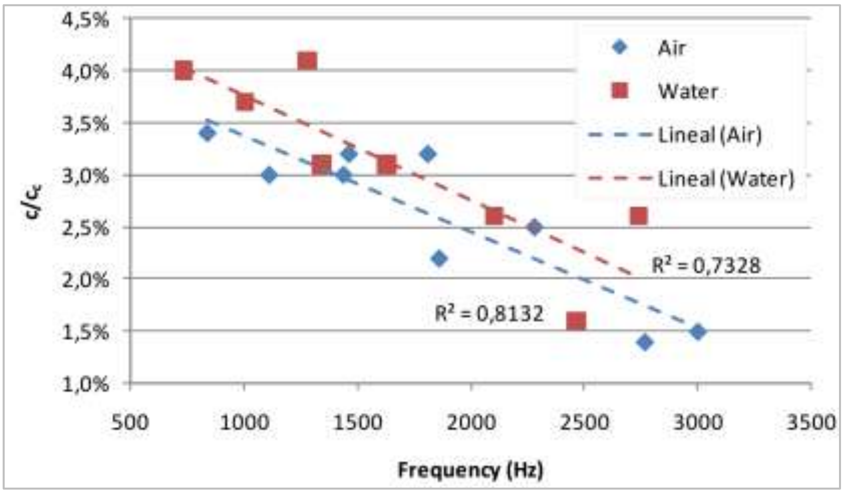

Figure 16: *Damping effects in air and water across natural frequencies for a pump-turbine runner model [54]. ccc = damping, ccc_ccc = critical damping.*

Hydrodynamic damping characterization in Francis turbines faces complexities due to differences between prototype and laboratory conditions. Local flow effects, such as those at blade leading edges, blade-band-crown junctions, and runner cones, may cause spatial variation in damping. Flow-dependent damping has also been documented in compressible turbomachinery blades [86]. Inaccurate damping estimates from isolated experiments can lead to critical design failures. Hence, comprehensive understanding of fluid damping under sediment erosion and flow variability is essential for reliable runner design and longevity.

International Journal of
Advanced Multidisciplinary Scientific Research (IJAMSR) ISSN:2581-4281

4. Fatigue Loading

In Section 2 on forced excitation, we discussed how Francis turbines are subjected to high amplitude dynamic pressures, which induce complex stress states on the runner blades. These stresses comprise both static stresses, due to steady-state mean pressure loads, and dynamic stresses, caused by cyclic pressure fluctuations arising from forced excitation phenomena. Experimental and numerical investigations indicate that stress concentrations are predominantly located at the leading and trailing edge T-junctions of the blades [98, 99].

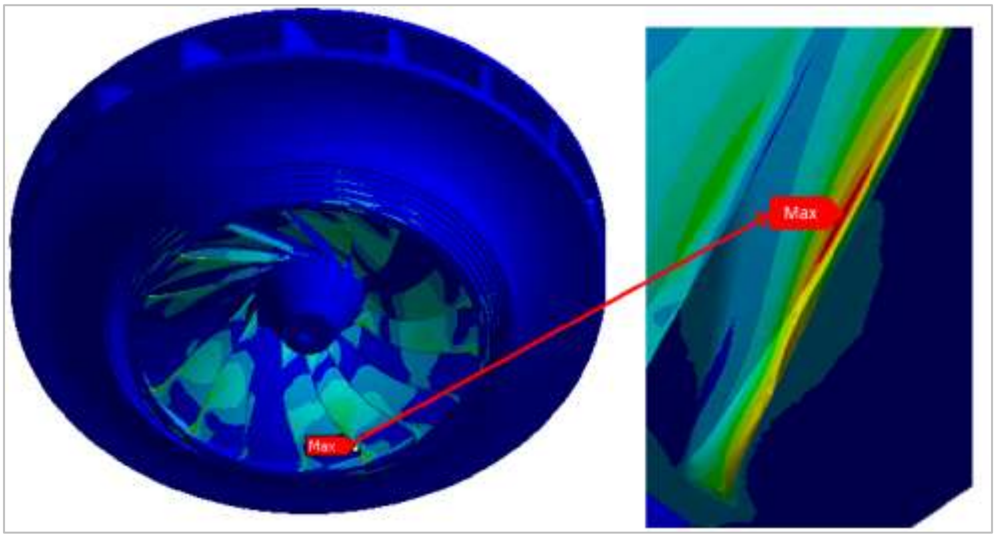

Figure 17: *Dynamic stress distribution on a Francis turbine runner under high-load conditions*

Figure 17 illustrates the Von Mises dynamic stress distribution on a Francis runner operating under high load. The highest stress levels occur at the T-junctions connecting the blades to the band and crown. Measuring stresses at these critical points is challenging due to the limitations in strain gauge size and protective coatings necessary for underwater applications. To enhance accuracy, steel templates are commonly employed for precise positioning of strain gauges—a technique widely used in industry [8]. These templates allow for rapid and reproducible placement across multiple blades.

In high-head Francis turbines, both static and dynamic stresses are significantly greater compared to mid- or low-head turbines, with stress magnitudes strongly dependent on the operating load. Figure 18 depicts the variation of principal and equivalent stresses at the blade trailing edge near the crown under different operating conditions. At the Best Efficiency Point (BEP) and stable operating regimes, the principal and Von Mises stresses are nearly identical. However, at high load conditions, the Von Mises equivalent stresses considerably exceed the principal stresses. Under part-load conditions (PL3 and PL4), the stresses converge again. Maximum static principal stresses in the runner reach approximately 25% of the material's yield strength, suggesting that fatigue damage primarily arises from the combined effect of residual, static, and dynamic stresses. The dynamic stresses notably influence crack initiation and propagation [9, 98, 100].

International Journal of
Advanced Multidisciplinary Scientific Research (IJAMSR) ISSN:2581-4281

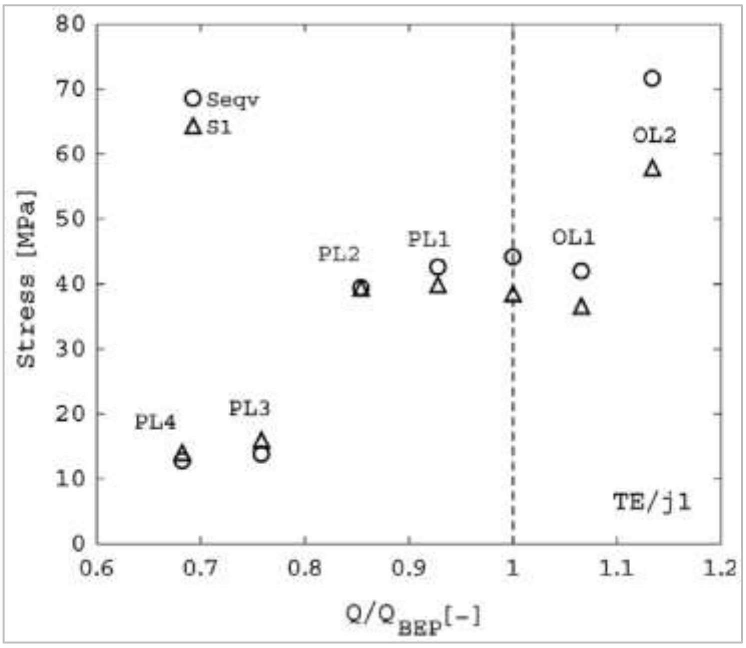

Figure 18: *Stress variation at blade trailing edge near crown of Francis turbine runner*

Francis turbines typically experience low cycle fatigue (LCF) during transient operating phases (less than 10^4 cycles) and high cycle fatigue (HCF) under steady-state operations (greater than or equal to 10^5 cycles). Increased transient operation and prolonged off-design running accelerate fatigue progression during the early operational life. One critical design parameter influencing fatigue life is the fillet radius at the blade T-junctions to the band and crown. Shape optimization studies demonstrate that increasing the fillet radius can improve fatigue life by a factor of 2 to 2.5 compared to conventional quarter-circular fillets [10].

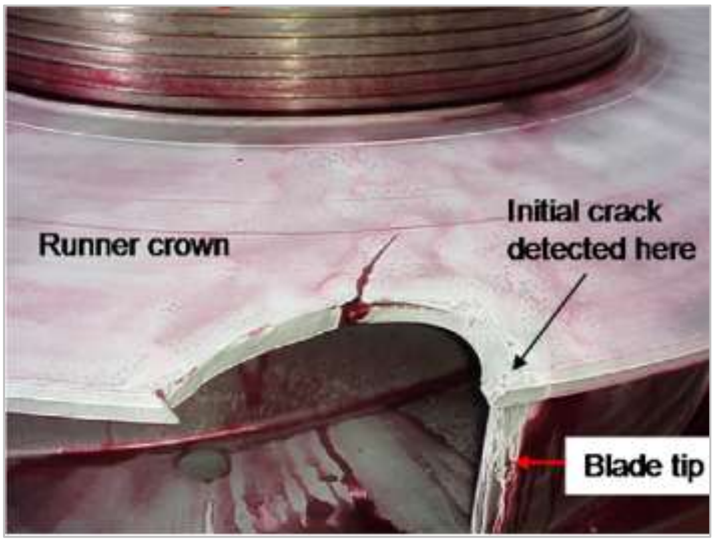

Figure 19: *Photograph of a fractured pump-turbine runner crown section*

International Journal of
Advanced Multidisciplinary Scientific Research (IJAMSR) ISSN:2581-4281

Figure 19 shows a fractured section of a pump-turbine runner crown. Detailed analysis revealed that failure was associated with elevated stress concentration at the blade leading edge T-junction. Increasing the fillet radius at this location effectively reduced stress concentrations. Moreover, the added mass effect—an influence of the surrounding water—significantly lowers the natural frequencies of the runner at certain nodal diameters, potentially aligning with excitation frequencies and leading to resonance. Such fatigue-induced failures are commonly reported in high-head hydraulic turbines, with cracks initiating predominantly from the leading edge T-junction [10-12, 18, 20, 102].

Fatigue damage is mainly driven by high amplitude dynamic stresses caused by rotor-stator interaction [25, 103]. Although numerical simulations accurately predict stress amplitudes under steady-state conditions, transient operations such as load variation, start-stop cycles, and full load rejection present more complex challenges. These transient conditions impose greater damage to runner blades than steady-state operations [4, 104]. For example, in high-head Francis turbines, blade loading rates during transient cycles can range from 10 to 50 MW/s, subjecting blades to alternating compressive and tensile stresses. Strain gauge measurements on a 600 MW Francis turbine indicate that compressive stresses dominate at the suction side trailing edge T-junctions, with stress magnitudes switching between tensile and compressive as load changes. Maximum tensile and compressive stresses reach approximately 100 MPa at full load and 230 MPa during total load rejection events [105].

Accurate prediction of pressure loading and its amplitude is critical to anticipating fatigue damage progression and preventing crack initiation. Due to the stochastic nature of load fluctuations, efficiently converting dynamic pressure fluctuations into structural deformations is essential. The Synchronous No-Load (SNL) operating condition is notably dynamic and requires thorough evaluation at the design phase [106-108].

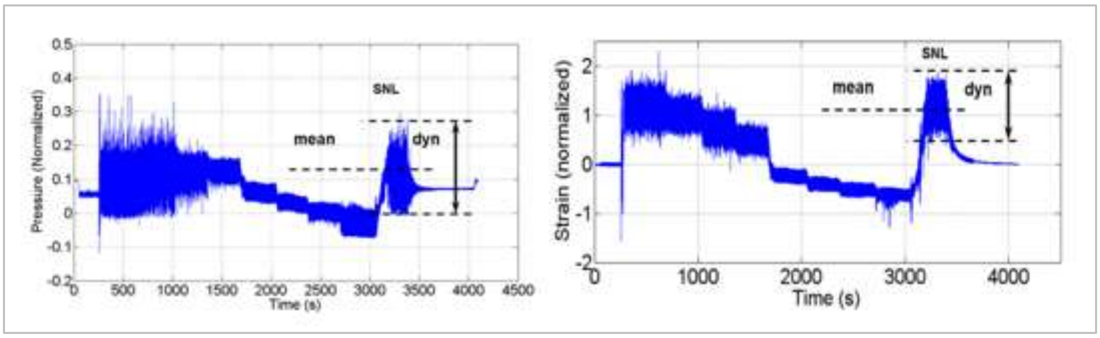

Figure 20: *Unsteady pressure and corresponding strain during start-stop cycle of a high-head Francis runner*

Figure 20 illustrates the variation of unsteady pressure and corresponding strain during a full start-stop cycle in a high-head Francis runner. The maximum pressure amplitude occurs during the SNL condition, where high-amplitude pressure pulsations combined with rapid strain changes pose serious risks to blade integrity, especially in load-peaking turbines [25, 40, 59, 103, 109].

Table 2: *Francis turbine runner types and operating ranges used for stress analysis*

Runner type	n_{ED}	Rated power category (MW)	Design type
A	0.4	200-400	Standard
B	0.4	>400	Wide operating range
C	0.3	200-400	Heavy duty
D	0.2	0-200	Standard
E	0.3	0-200	Standard

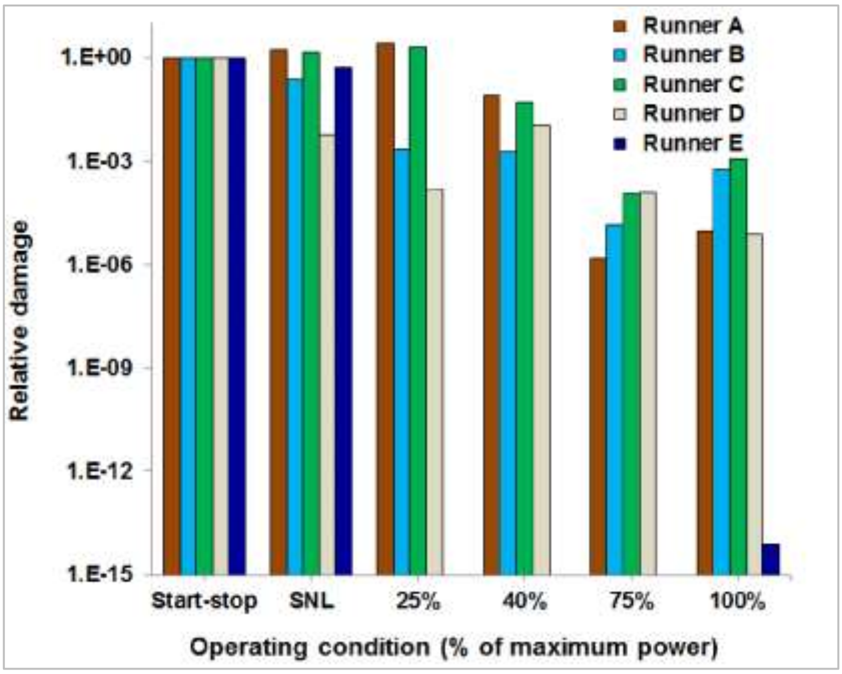

Figure 21: *Relative fatigue damage factor comparison among different Francis runner types*

Figure 21 compares relative fatigue damage factors in Francis runners across various categories (as detailed in Table 2). Maximum damage consistently occurs during start-stop and SNL operations. Notably, a single start-stop cycle can cause more fatigue damage than several days of steady-state operation. Frequent start-stop cycles may reduce runner life by several years, emphasizing the importance of operational strategies that minimize the number of start-stops. However, continuous operation at SNL conditions incurs additional costs due to water loss and increased component wear. The first natural frequency of the runner may sometimes be below the forced excitation frequency, increasing the risk of resonant vibrations and catastrophic failure if spinning beyond structural limits [99].

These observations underscore the critical need for detailed fluid-structure interaction analysis in the presence of sediment erosion, as sediment particles exacerbate surface wear and modify hydrodynamic loading patterns. Understanding these coupled interactions is essential for predicting fatigue life and informing design modifications or operational guidelines.

International Journal of
Advanced Multidisciplinary Scientific Research (IJAMSR) ISSN:2581-4281

Gagnon et al. [111] conducted comprehensive studies addressing transient conditions such as start-stop, SNL, and load rejection with full or partial air admission. Their work highlights the necessity for periodic review of guide vane operation schemes to manage fatigue loading effectively. The economic benefits of such optimization far outweigh the costs related to blade damage. Furthermore, air admission systems—traditionally considered safety devices—should be viewed as tools to prolong runner life by mitigating unsteady pressure fluctuations during transient cycles [111].

Overall, hydraulic turbines operate in complex fluid-structure environments where the surrounding water significantly affects structural dynamic behavior. The added mass effect can reduce natural frequencies by up to 50% compared to air conditions. Additionally, Von Karman vortex shedding at blade edges may induce lock-in phenomena when vortex shedding frequencies approach structural natural frequencies, leading to large amplitude vibrations and fatigue damage. The confined runner environment—with narrow gaps between rotating and stationary components—can further amplify vibrations through hydroelastic instabilities, particularly in labyrinth seals and close guide vanes, sometimes causing structural failure [Hübner, 2010 #176; Hubner, 2008 #363; Paidoussis, 1998 #404].

5. Quality and Trust in Numerical Studies

Over the last three decades, numerical techniques have significantly advanced the design and analysis of hydraulic turbines. In the current research landscape, nearly all fluid-structure interaction (FSI) investigations, especially those concerning Francis turbines, rely heavily on computational modeling. However, the reliability of many such numerical simulations remains limited due to insufficient verification and validation efforts.

To ensure the credibility of FSI analyses under **sediment erosion conditions**, especially in Francis turbines, rigorous assessment of the selected numerical methods is imperative. Verification and validation (V&V) procedures must be integrated into the modeling workflow to ensure the accuracy of results and to support meaningful design decisions.

5.1 Mesh Discretization and Error Assessment

A common focus of numerical studies in FSI is the evaluation of added mass effects through natural frequency and mode shape analysis. These analyses require accurate discretization of the computational domain using mesh elements. Mesh quality, type, and resolution directly impact the solution's convergence and reliability.

Richardson extrapolation techniques are frequently used to estimate discretization error and mesh convergence. For example, studies on model Francis runners have shown the importance of selecting optimal mesh density and type. As shown in **Figure 1**, a mesh convergence study was performed using both tetrahedral and hexahedral meshes. Below 4,000 nodes, tetrahedral meshes produced significantly larger deviations. A mesh-independent solution was achieved with approximately 8,529 nodes for both mesh types, with hexahedral meshes showing faster convergence.

International Journal of
Advanced Multidisciplinary Scientific Research (IJAMSR) ISSN:2581-4281

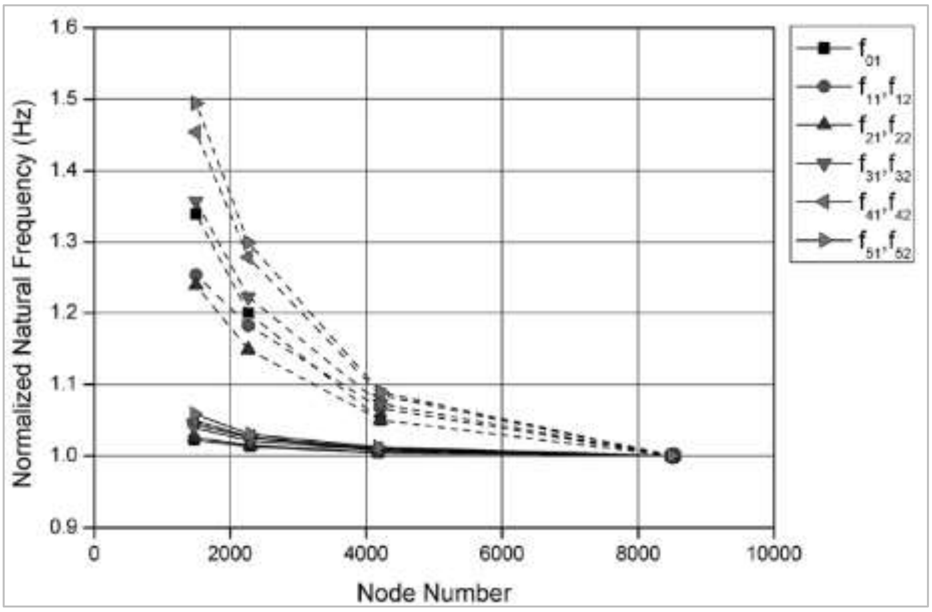

Figure 22: *Mesh sensitivity analysis of a model Francis runner*

Despite the prevalent use of tetrahedral meshes, they are more computationally intensive than hexahedral meshes. Nonetheless, sensitivity analyses often reveal no major discrepancies between the two, provided adequate node density is maintained. For FSI studies under sediment erosion, sensitivity analyses should not only address natural frequency but also parameters such as mode shape accuracy, Young's modulus, nodal diameter/circle, and structure deformation, especially at critical erosion-prone regions like blade fillets.

Proper radial resolution near fillet radii is essential to capture stress concentrations exacerbated by erosion. As highlighted in several studies, mesh quality—particularly element shape and node spacing normal to the FSI interface—can significantly influence the stress results. Low-quality meshes tend to underestimate stress values, leading to potentially unsafe designs.

5.2 Temporal Accuracy and Boundary Conditions

Most current FSI simulations are carried out under steady-state assumptions. However, **unsteady simulations** are crucial for capturing transient behavior due to sediment-induced erosion and dynamic pressure fluctuations. Time step size plays a critical role; overly large steps introduce numerical error, while very small steps increase computational cost. A balance must be struck to ensure both accuracy and efficiency.

Boundary conditions derived from experimental data are typically used for validation. However, these data carry inherent uncertainties due to measurement errors and varying test conditions. Consequently, numerical outcomes are influenced by compounded uncertainties—arising from mesh convergence, input boundary conditions, vibration and strain measurement inaccuracies, and the CFD-derived pressure fields used in structural simulations.

International Journal of
Advanced Multidisciplinary Scientific Research (IJAMSR) ISSN:2581-4281

For example, when performing stress analysis of a Francis runner, pressure loads obtained from CFD simulations at various operating conditions are applied to the structure. Reported errors in pressure amplitudes may range from 5% to 40%, further complicating structural response predictions. Hence, a detailed quantification of error sources is essential, and appropriate **safety factors** should be employed, particularly in prototype development.

5.3 Computational Requirements and Practical Challenges

One of the key limitations in high-fidelity FSI simulations—especially for sediment-laden flows—is the demand for substantial computational resources. Accurate spatial and temporal resolution requires fine mesh and small-time steps, which are computationally expensive.

As illustrated in **Figure 2**, two-way coupled FSI simulations require orders of magnitude more computational effort than simplified one-way approaches. Given the challenges in resource availability, researchers must make strategic modeling choices. These include deciding when to use:

1. One-way vs. two-way coupling,
2. Steady, quasi-steady, or unsteady simulations,
3. Dynamic mesh simulations for full-turbine geometries,
4. Representative operating conditions for broader generalization.

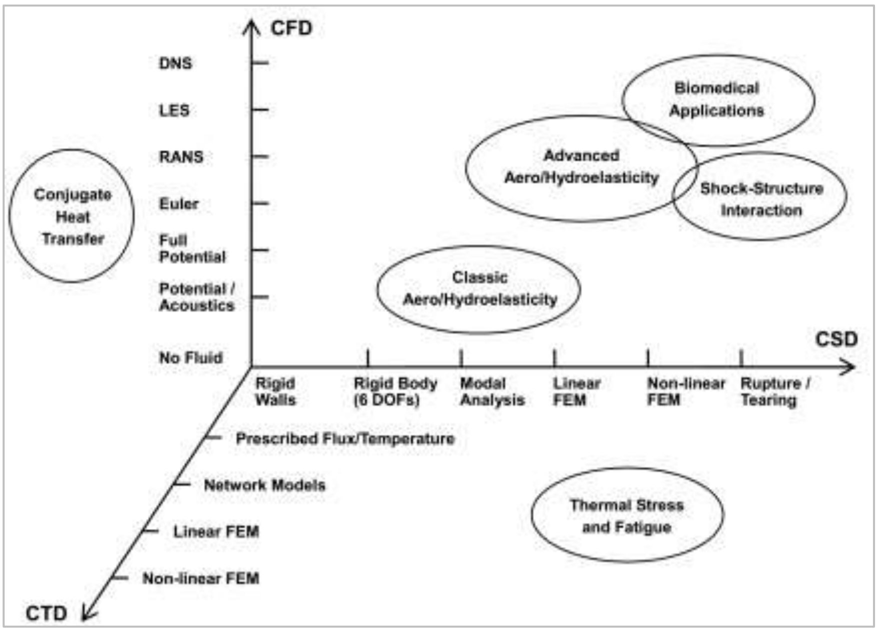

Figure 23: *Computational cost vs. modeling complexity in coupled simulations*

Hydropower industries are increasingly shifting towards **virtual testing** and multidisciplinary design optimization (MDO) of turbine components. This trend emphasizes the importance of robust simulation frameworks validated by experimental data, ideally collected at both model and prototype scales.

IJAMSR

International Journal of Advanced Multidisciplinary Scientific Research (IJAMSR) ISSN:2581-4281

5.4 Conclusion

Building trust in numerical studies of FSI in Francis turbines, particularly under sediment erosion conditions, hinges on comprehensive verification, validation, and sensitivity analyses. Special attention must be given to mesh quality, time step control, and accurate boundary conditions. Uncertainties must be quantified and mitigated through safety factors and error propagation studies. As computational resources become more accessible, high-fidelity simulations—supplemented by strategic simplifications—will play an increasingly vital role in turbine design and failure prevention in erosion-prone environments.

6. Prototype Transposition under Sediment-Laden Conditions

Model testing is indispensable for mapping hydraulic behaviour over the complete operating range, yet it remains inadequate for capturing the full fluid-structure response—especially when sediment erosion is present. Scaling laws cannot faithfully reproduce prototype-scale sound speed, added mass, or hydro-acoustic characteristics, all of which are altered once sediment roughens flow passages. Parameters that *must* be assessed on the full-scale turbine include in-situ flow velocity at strategic runner locations, the coupled dynamic response of the runner–shaft–generator train, and the resonant frequencies of the integrated rotating assembly [105].

Structural similarity is further compromised by material differences: bronze model runners contrast with prototype runners machined or welded from martensitic/austenitic stainless steels (12–17 % Cr, e.g., 16Cr-5Ni) [10]. Under abrasive flow, erosion-induced surface pitting can locally thin the stainless-steel blades, shifting both mass distribution and stiffness and thereby modifying modal properties. Vibrations of submerged components—stay vanes, guide vanes and runner—can therefore reach critical amplitudes if erosion-altered damping or stiffness is ignored.

Encouragingly, several characteristics *do* transpose: the family of mode shapes (nodal diameters) observed on models generally reappears on prototypes, and hydrodynamic damping trends remain qualitatively similar. Damping peaks at the best-efficiency point (BEP) but falls sharply under part- and high-load conditions, where abrasive sediment concentrations are often highest. Establishing quantitative relations between flow velocity, sediment concentration, and damping for both scales would refine erosion-aware design factors.

7. Future Directions for Fluid-Structure–Erosion Coupling in Hydropower

The past five years have witnessed rapid adoption of two-way coupled CFD–FEA techniques for Francis-runner optimisation. Yet most work still concentrates on frequency-reduction ratios derived from dry-modal analyses. To progress toward erosion-resilient designs, three complementary research strands are required:

1. **Mode-shape evolution and nodal-line migration.** Sediment scouring preferentially affects leading edges and crown/band fillets, locations critical for bending-torsion coupling. Tracking how these geometric changes shift mode shapes—and therefore excitation overlap with rotor-stator interaction (RSI) harmonics—will sharpen life predictions.

IJAMSR

International Journal of
Advanced Multidisciplinary Scientific Research (IJAMSR) ISSN:2581-4281

2. **Hydrodynamic damping under abrasive multiphase flow.** Hydro-foil experiments show damping rising almost linearly with flow velocity up to ~40 m s^{-1}, typical of mid-/high-head turbines. Whether entrained silt enhances or suppresses this damping remains unanswered. Key questions include:

- How does damping vary across BEP, off-design, runaway and synchronous-no-load (SNL) regimes with realistic sediment loads?
- Does blade-only testing misrepresent damping of the full runner–and–hub system?
- Can strategically thickened leading-edge weld overlays recover damping for dominant bending and torsional modes without excessive mass penalty?

3. **Blade flutter and added-mass interaction in eroding runners.** High-amplitude crown deformation correlates with flutter at the trailing edge—yet no systematic flutter study exists for hydraulic turbines. Recent incompressible-flow flutter solvers could be adapted to sediment-laden water by incorporating variable density and viscosity fields. Controlling mode shape (rather than merely reducing frequency) via targeted stiffness additions or composite patches presents a promising mitigation path [130].

Transient events—start-ups, load rejections, and SNL passages—impose the severest combined hydrodynamic and erosion stresses. Strain-gauge campaigns [59] confirm that fatigue damage accumulates fastest during these manoeuvres. High-fidelity transient FSI, however, is still hampered by mesh deformation challenges, especially when eroded geometries evolve during the simulation. Robust remeshing or immersed-boundary strategies are needed to keep computational cost practical.

Prototype extrapolation efforts are emerging: Huang et al. [40], Coutu et al. [109] and Rodriguez et al. [38, 53] compare runners across operating points, offering initial guidance on added-mass and damping scaling for specific-speed classes. Extending these comparisons to sediment-prone sites will accelerate validation of erosion-aware similitude rules.

8 Summary and Research Gaps

This review has revisited fluid-structure interaction (FSI) phenomena in Francis turbines through the lens of **sediment erosion**, outlining the outstanding challenges that must be solved to design durable, flexible units for sediment-rich rivers.

- **Forced excitation vs. natural frequencies.** Mid-/high-head machines, already sensitive to RSI, face amplified uncertainty once erosion changes blade mass and stiffness. Numerical amplitude predictions show up to 40 % deviation from experiments—tolerable only with conservative design margins that eroded blades may quickly violate.
- **Added-mass in flowing, abrasive water.** Classic still-water corrections reduce natural frequencies by as much as 60 %, but flowing water, cavitation pockets, and sediment concentration all modulate this effect. Hydro-foil data suggest still-water estimates overshoot by 10–15 %. Prototype-scale studies are essential to pin down erosion-corrected added-mass coefficients.

International Journal of Advanced Multidisciplinary Scientific Research (IJAMSR) ISSN:2581-4281

- **Hydrodynamic damping and blade flutter.** Both remain sparsely researched. Preliminary tests hint at beneficial damping growth with velocity, yet the roles of cavitation nuclei and particle loading are unquantified. Flutter, long acknowledged in aero- and gas-turbines, could explain unexpected vibration spikes in eroding runners but has not been systematically mapped.
- **Fatigue and crack initiation.** Dynamic stresses concentrate at T-junctions and eroded leading/trailing edges. Catastrophic field failures (e.g., SM-3, unit-1, Hydro-Québec) highlight how thin safety margins become when erosion, higher power density, and wider operating ranges intersect. Reliable multi-axial fatigue models that integrate evolving geometry are still lacking.
- **Cost-effective numerical workflows.** State-of-the-art two-way FSI with moving meshes is computationally heavy; yet simpler methods can reach similar accuracy if calibrated. Establishing when advanced approaches are truly warranted—and how their findings transpose to prototypes—will save both time and resources.

References

1. Sawin, J. L., Sverrisson, F., & Rickerson, W. (2015). *Renewables 2015: Global status report* (L. Mastny, Ed.). Renewable Energy Policy Network for the 21st Century (REN21 Secretariat).
2. Daugherty, R. L. (1920). *Hydraulic turbines, with a chapter on centrifugal pumps* (1st ed.). McGraw-Hill.
3. Deschênes, C., Fraser, R., & Fau, J.-P. (2002, October). New trends in turbine modelling and partnership strategies. In *Proceedings of IGHEM* (pp. 1–12). Toronto, Canada.
4. Trivedi, C., Gandhi, B., & Cervantes, M. (2013). Effect of transients on Francis-turbine runner life: A review. *Journal of Hydraulic Research, 51*(2), 121–132. https://doi.org/10.1080/00221686.2012.732971
5. Dorji, U., & Ghomashchi, R. (2014). Hydro-turbine failure mechanisms: An overview. *Engineering Failure Analysis, 44*, 136–147. https://doi.org/10.1016/j.engfailanal.2014.04.013
6. Keck, H., Weiss, T., Michler, W., & Sick, M. (2009). Recent advances in dynamic analysis of water turbines. *Proceedings of the Institution of Mechanical Engineers, Part A: Journal of Power and Energy, 223*, 415–427. https://doi.org/10.1243/09576509JPE578
7. Magnoli, M. V. (2014). *Numerical simulation of pressure oscillations in large Francis turbines at partial and full load and their influence on runner structure and fatigue life* [Doctoral dissertation, Technische Universität München].
8. Seidel, U., Hübner, B., Löfflad, J., & Faigle, P. (2012). Evaluation of RSI-induced stresses in Francis runners. *IOP Conference Series: Earth and Environmental Science, 15*(5), 052010. https://doi.org/10.1088/1755-1315/15/5/052010
9. Xiao, R., Wang, Z., & Luo, Y. (2008). Dynamic stresses in a Francis-turbine runner using fluid–structure interaction. *Tsinghua Science and Technology, 13*(5), 587–592.
10. Huth, H.-J. (2005). *Fatigue design of hydraulic turbine runners* [Doctoral dissertation, Norwegian University of Science and Technology].

I J A M S R

International Journal of
Advanced Multidisciplinary Scientific Research (IJAMSR) ISSN:2581-4281

11. Seidel, U., Mende, C., Hübner, B., Weber, W., & Otto, A. (2014). Dynamic loads in Francis runners and their impact on fatigue life. *IOP Conference Series: Earth and Environmental Science, 22*(3), 032054. https://doi.org/10.1088/1755-1315/22/3/032054
12. Thibault, D., Gagnon, M., & Godin, S. (2014). Connecting metallurgy to fatigue reliability in hydraulic-turbine runners. *IOP Conference Series: Earth and Environmental Science, 22*(1), 012019. https://doi.org/10.1088/1755-1315/22/1/012019
13. Keck, H., & Sick, M. (2008). Thirty years of numerical flow simulation in hydraulic turbomachinery. *Acta Mechanica, 201*, 211–229. https://doi.org/10.1007/s00707-008-0060-4
14. Bergmann-Paulsen, J. (2012). *Fluid–structure interaction analysis of a Francis turbine* [Master's thesis, Norwegian University of Science and Technology].
15. Roth, S., Hasmatuchi, V., Botero, F., Farhat, M., & Avellan, F. (2010). Fluid–structure coupling in the guide-vane cascade of a pump-turbine scale model. *IOP Conference Series: Earth and Environmental Science, 12*(1), 012074. https://doi.org/10.1088/1755-1315/12/1/012074
16. Sarpkaya, T. (2004). The intrinsic nature of vortex-induced vibrations: A critical review. *Journal of Fluids and Structures, 19*, 389–447. https://doi.org/10.1016/j.jfluidstructs.2004.02.005
17. Egusquiza, E., Valero, C., Liang, Q., Coussirat, M., & Seidel, U. (2009, August). Fluid added-mass effects on the modal response of a pump-turbine impeller. In *Proceedings of the ASME 2009 International Design Engineering Technical Conferences* (pp. 715–724). San Diego, CA. https://doi.org/10.1115/DETC2009-86830
18. Trudel, A., & Sabourin, M. (2014). Metallurgical and fatigue evaluations of welds in cast welded hydraulic-turbine runners. *IOP Conference Series: Earth and Environmental Science, 22*(1), 012015. https://doi.org/10.1088/1755-1315/22/1/012015
19. Zhou, L. J., Wang, Z. W., Xiao, R. F., & Luo, Y. Y. (2007). Dynamic stress analysis of Kaplan-turbine blades. *Engineering Computations, 24*(7), 753–762. https://doi.org/10.1108/02644400710833288
20. Gagnon, M., Tahan, S. A., Bocher, P., & Thibault, D. (2012). High-cycle-fatigue initiation and its role in Francis-runner reliability. *IOP Conference Series: Earth and Environmental Science, 15*(2), 022005. https://doi.org/10.1088/1755-1315/15/2/022005
21. Coutu, A., Proulx, D., Coulson, S., & Demers, A. (2004, August). Dynamic assessment of high-head Francis turbines. In *HydroVision 2004* (Paper 13). Montréal, Canada.
22. Coutu, A., Roy, M. D., Monette, C., & Nennemann, B. (2008, October). Rotor–stator interactions in high-head Francis runners: Field experience. In *Proceedings of the 24th IAHR Symposium on Hydraulic Machinery and Systems* (Paper 10). Foz do Iguaçu, Brazil.
23. Egusquiza, E., Valero, C., Huang, X. X., Jou, E., Guardo, A., & Rodriguez, C. (2012). Failure analysis of a large pump-turbine runner. *Engineering Failure Analysis, 23*, 27–34. https://doi.org/10.1016/j.engfailanal.2012.01.012
24. Frunzăverde, D., Muntean, S., Mărginean, G., Campian, V., Marșavina, L., Terzi, R., et al. (2010). Failure investigation of a Francis-turbine runner. *IOP Conference Series: Earth and Environmental Science, 12*(1), 012115. https://doi.org/10.1088/1755-1315/12/1/012115

International Journal of Advanced Multidisciplinary Scientific Research (IJAMSR) ISSN:2581-4281

25. Nennemann, B., Morissette, J.-F., Chamberland-Lauzon, J., Monette, C., Braun, O., Melot, M., et al. (2014). Predicting dynamic pressure and stress at no-load operation in hydraulic turbines: Current challenges. *IOP Conference Series: Earth and Environmental Science, 22*(3), 032055. https://doi.org/10.1088/1755-1315/22/3/032055
26. Jonsson, P. P., Mulu, B. G., & Cervantes, M. J. (2012). Experimental investigation of a Kaplan draft tube: Part II—Off-design conditions. *Applied Energy, 94*, 71–83. https://doi.org/10.1016/j.apenergy.2012.01.032
27. Doerfler, P., & Ruchonnet, N. (2012). Statistical evaluation of draft-tube pressure pulsations. *IOP Conference Series: Earth and Environmental Science, 15*(6), 062002. https://doi.org/10.1088/1755-1315/15/6/062002
28. Susan-Resiga, R., Câmpian, V., Dumbravă, C., & Muntean, A. C. S. (2013). In-situ unsteady-pressure measurements on the draft-tube cone of a Francis turbine with air injection across an extended operating range. *Calcutta Institute of Engineering and Management Technical Journal, 25*, Article e25.
29. Nicolet, C., Zobeiri, A., Maruzewski, P., & Avellan, F. (2010). Experimental study of the upper part-load vortex rope in a Francis turbine. *IOP Conference Series: Earth and Environmental Science, 12*(1), 012053. https://doi.org/10.1088/1755-1315/12/1/012053
30. Dörfler, P., Sick, M., & Coutu, A. (2013). *Flow-induced pulsation and vibration in hydroelectric machinery* (1st ed.). Springer.
31. Ausoni, P., Farhat, M., Escaler, X., Egusquiza, E., & Avellan, F. (2007). Cavitation effects on von Kármán vortex shedding and the resulting hydrofoil vibrations. *Journal of Fluids Engineering, 129*(8), 966–973. https://doi.org/10.1115/1.2746907
32. Zobeiri, A., Ausoni, P., Avellan, F., & Farhat, M. (2012). Reduction of vortex-induced vibration with an oblique trailing edge on a hydrofoil. *Journal of Fluids and Structures, 32*, 78–89. https://doi.org/10.1016/j.jfluidstructs.2011.12.003
33. Ohashi, H. (1994). Pump failure due to rotor–stator interaction: A case study. *International Journal of Rotating Machinery, 1*(1), 53–60. https://doi.org/10.1155/S1023621X94000059
34. Trivedi, C., Cervantes, M., Gandhi, B., & Dahlhaug, O. G. (2013). Experimental and numerical analysis of a high-head Francis turbine at multiple operating points. *Journal of Fluids Engineering, 135*(11), 111102-1–111102-17. https://doi.org/10.1115/1.4024805
35. Zobeiri, A. (2009). *Time-dependent flow phenomena in Francis turbines and pump-turbines: Rotor–stator interaction and precessing vortex rope* [Doctoral dissertation, École Polytechnique Fédérale de Lausanne].
36. Nicolet, C., Ruchonnet, N., Alligné, S., Koutnik, J., & Avellan, F. (2010). Hydroacoustic simulation of rotor–stator interaction in resonance in a Francis pump-turbine. *IOP Conference Series: Earth and Environmental Science, 12*(1), 012005. https://doi.org/10.1088/1755-1315/12/1/012005
37. Zobeiri, A., Kueny, J.-L., Farhat, M., & Avellan, F. (2006, October). Pressure fluctuations in the distributor channel of a pump-turbine operating in generating mode. In *Proceedings of the 23rd IAHR Symposium* (pp. 1–10). Yokohama, Japan.

38. Rodriguez, C. G., Egusquiza, E., & Santos, I. F. (2007). Frequency content of vibration induced by rotor–stator interaction in a centrifugal pump-turbine. *Journal of Fluids Engineering, 129*(11), 1428–1435. https://doi.org/10.1115/1.2786489
39. Hasmatuchi, V. (2012). *Hydrodynamics of a pump-turbine operating at off-design conditions in generating mode* [Doctoral dissertation, École Polytechnique Fédérale de Lausanne].
40. Huang, X., Chamberland-Lauzon, J., Oram, C., Klopfer, A., & Ruchonnet, N. (2014). Fatigue analyses of prototype Francis runners using site measurements and simulations. *IOP Conference Series: Earth and Environmental Science, 22*(1), 012014. https://doi.org/10.1088/1755-1315/22/1/012014
41. Jošt, D., Škerlavaj, A., Morgut, M., Mežnar, P., & Nobile, E. (2015). CFD simulation of flow in a high-head Francis turbine: Efficiency, rotor–stator interaction and draft-tube vortices. *Journal of Physics: Conference Series, 579*, 012006. https://doi.org/10.1088/1742-6596/579/1/012006
42. Roache, P. J. (1997). Quantifying uncertainty in computational fluid dynamics. *Annual Review of Fluid Mechanics, 29*, 123–160. https://doi.org/10.1146/annurev.fluid.29.1.123
43. Roache, P. J. (2009). Validation in perspective: What does it mean? *Journal of Fluids Engineering, 131*(3), 034503. https://doi.org/10.1115/1.3077134
44. Celik, I. B., Ghia, U., Roache, P. J., & Freitas, C. J. (2008). Estimating and reporting discretization uncertainty in CFD. *Journal of Fluids Engineering, 130*(7), 078001. https://doi.org/10.1115/1.2960953
45. Stern, F., Wilson, R., & Shao, J. (2006). Quantitative verification and validation of CFD simulations and certification of CFD codes. *International Journal for Numerical Methods in Fluids, 50*(11), 1335–1355. https://doi.org/10.1002/fld.1090
46. Leonard, A., & Roshko, A. (2001). Selected aspects of flow-induced vibration. *Journal of Fluids and Structures, 15*, 415–425. https://doi.org/10.1006/jfls.2000.0360
47. Williamson, C. H. K., & Govardhan, R. (2008). Recent advances in vortex-induced vibrations: A concise review. *Journal of Wind Engineering and Industrial Aerodynamics, 96*, 713–735. https://doi.org/10.1016/j.jweia.2007.06.019
48. Hübner, B., Seidel, U., & Roth, S. (2010). Predicting turbine-component dynamics through fluid–structure coupling. *IOP Conference Series: Earth and Environmental Science, 12*(1), 012009. https://doi.org/10.1088/1755-1315/12/1/012009
49. Liang, Q. W., Rodriguez, C. G., Egusquiza, E., Escaler, X., Farhat, M., & Avellan, F. (2007). CFD study of fluid added-mass effects on a Francis-runner. *Computers & Fluids, 36*, 1106–1118. https://doi.org/10.1016/j.compfluid.2006.08.007
50. Lais, S., Liang, Q., Henggeler, U., Weiss, T., Escaler, X., & Egusquiza, E. (2009). Dynamic analysis of Francis runners: Experiments and simulation. *International Journal of Fluid Machinery and Systems, 2*(4), 303–314. https://doi.org/10.5293/IJFMS.2009.2.4.303
51. Valero, C., Huang, X., Egusquiza, E., Farhat, M., & Avellan, F. (2010). Modal behaviour of a reduced-scale pump-turbine impeller. Part 2: Numerical simulation. *IOP Conference Series: Earth and Environmental Science, 12*(1), 012117. https://doi.org/10.1088/1755-1315/12/1/012117

I J A M S R

International Journal of Advanced Multidisciplinary Scientific Research (IJAMSR) ISSN:2581-4281

52. Flores, M., Urquiza, G., & Rodríguez, J. M. (2012). Fatigue analysis of a hydraulic Francis-turbine runner. *World Journal of Mechanics*, *2*(1), 28–34. https://doi.org/10.4236/wjm.2012.21004
53. Rodriguez, C. G., Egusquiza, E., Escaler, X., Liang, Q. W., & Avellan, F. (2006). Added-mass effects on a Francis-runner in still water: Experimental investigation. *Journal of Fluids and Structures*, *22*(5), 699–712. https://doi.org/10.1016/j.jfluidstructs.2006.04.001
54. Escaler, X., Hütter, J. K., Egusquiza, E., Farhat, M., & Avellan, F. (2010). Modal behaviour of a reduced-scale pump-turbine impeller. Part 1: Experiments. *IOP Conference Series: Earth and Environmental Science*, *12*(1), 012116. https://doi.org/10.1088/1755-1315/12/1/012116
55. Coutu, A., Seeley, C., Monette, C., Nennemann, B., & Marmont, H. (2012). Measuring damping in flowing water. *IOP Conference Series: Earth and Environmental Science*, *15*(6), 062060. https://doi.org/10.1088/1755-1315/15/6/062060
56. Jeffers, T. R., Kielb, J. J., & Abhari, R. S. (2000, May). Measuring blade damping with piezoelectric actuators: A novel technique. In *ASME Turbo Expo 2000—Power for Land, Sea, and Air* (Paper 2000-GT-0359). Munich, Germany. https://doi.org/10.1115/2000-GT-0359
57. Wilkie, W. K., Inman, D. J., Lloyd, J. M., & High, J. W. (2006). Anisotropic laminar piezocomposite actuators with machined PMN-PT single-crystal fibres. *Journal of Intelligent Material Systems and Structures*, *17*(1), 15–28. https://doi.org/10.1177/1045389X06055891
58. He, L. Y., He, Y., Luo, Y. Y., & Wang, Z. W. (2013). Fluid added-mass effects in the modal response of a pump-turbine runner. *Materials Science and Engineering Conference Series*, *52*, 022038. https://doi.org/10.1088/1757-899X/52/2/022038
59. Huang, X., Oram, C., & Sick, M. (2014). Static and dynamic stress analyses of a prototype high-head Francis runner from site measurements. *IOP Conference Series: Earth and Environmental Science*, *22*(3), 032052. https://doi.org/10.1088/1755-1315/22/3/032052
60. Schmucker, H., Flemming, F., & Coulson, S. (2010). Two-way coupled fluid-structure-interaction simulation of a propeller turbine. *IOP Conference Series: Earth and Environmental Science*, *12*(1), 012011. https://doi.org/10.5293/IJFMS.2010.3.4.342